P5.8 POLARIMETRIC METHOD FOR BRIGHT BAND DETECTION

S. E. Giangrande and A.V. Ryzhkov
Cooperative Institute for Mesoscale Meteorological Studies, University of Oklahoma

1. Introduction

A fuzzy logic approach has been adopted for operational polarimetric hydrometeor classification with the NSSL KOUN prototype polarimetric WSR-88D. This technique exhibits good performance for the discrimination between meteorological and non-meteorological echoes, as well as the improved detection of hail. However, distinguishing between light rain and dry aggregated snow is challenging because of small polarimetric contrasts between these media. Therefore, identification of the melting layer is necessary to delineate liquid and frozen particles for successful application of the fuzzy logic approach. Establishing the location of the melting layer has additional implications for data quality and proper application of radar rainfall algorithms.

This paper examines a technique for melting layer detection with dual-polarization weather radars. Recent studies by Ikeda and Brandes (2003) focus on freezing level detection using polarimetric signatures. However, the transition from rain to snow may occur at heights well below the 0°C isotherm. Thus, the focus of the study is to estimate the height of the bottom of the melting layer for proper rain/snow distinction rather than the freezing level.

2. Description of the method

The technique for bright band detection takes a slightly different approach than the one suggested by Ikeda and Brandes (2003). The latter utilizes radar reflectivity Z, cross-correlation coefficient ρ_{HV}, and linear depolarization ratio L_{DR}. According to Ikeda and Brandes (2003), the observed profiles of the three variables are matches with model profiles. Our technique makes use of Z, differential reflectivity Z_{DR}, and ρ_{HV} (L_{DR} is not available for the KOUN radar) and does not involve matching the observed and model profiles.

It is well known that the bright band is characterized by a drop in ρ_{HV} associated with Z and Z_{DR} peaks. These signatures, however, usually do not coincide in height. Most often, the maximum of Z is observed at a higher altitude than the maximum of Z_{DR} and minimum of ρ_{HV}. Among these three, the ρ_{HV} signature has the most useful discriminative power for bright band detection.

For each slant radar beam, the suggested procedure starts with identification of range gates in which ρ_{HV} is between 0.90 and 0.97. If maximum values of Z between 30 and 47 dBZ and Z_{DR} exceeding 0.8 dB are observed in close proximity to the gate where ρ_{HV} resides in this interval, the range gate is classified as 'bright band'.

Radial profiles of Z, Z_{DR}, ρ_{HV} and differential phase Φ_{DP} (which is not used for detection) in Fig. 1 illustrate bright band signatures at the elevation angle of 4.5° in the case of widespread stratiform rain on 4 June 2003 (1330 UTC). A pronounced drop in ρ_{HV} below 0.97 at the slant range of about 30 km (2.2 km height) marks the bottom of the melting layer. This ρ_{HV} drop is associated with well-defined maximums in Z and Z_{DR} at slightly higher altitudes. At larger slant ranges (higher altitudes), ρ_{HV} returns to higher values while Z and Z_{DR} acquire values typical for dry aggregated snow.

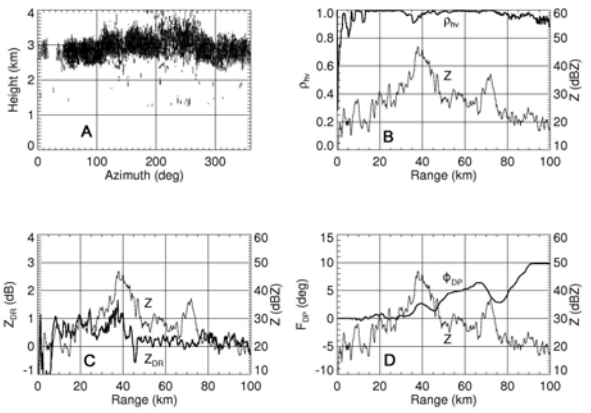

Fig. 1. (A) Results of polarimetric bright band detection for 4 June 2003 (1330 UTC). Slant range dependencies of (B) $\rho_{HV,}$ (C) Z_{DR}, and (D) Φ_{DP} for the 180° azimuth at 4.5° are also displayed.

The results of bright band identification at 5 elevation angles between 4.5° and 8.7° are summarized in Fig. 1A as a height-azimuth dependence. The bright band signature is not identified in certain azimuthal directions due to an absence of echo. In the 'stratiform echo', the height of the bright band signature indicating wet snow varies mainly between 2.4 and 3.6 km, with some hint of an azimuthal modulation. Slightly higher

Corresponding author address: Scott Giangrande, CIMMS/NSSL, 1313 Halley Circle, Norman, OK 73069
Email: Scott.Giangrande@noaa.gov

bright band signatures are observed in the sector where the highest surface temperatures are recorded (south and west). The bottom of the melting layer (or Bright band signature) is approximately 0.4 km lower in northerly directions. Variability generally corresponds to the direction of intense convective cells. Changes in the depth of these signatures may be associated with the presence of small hail embedded in heavy precipitation (can exhibit polarimetric characteristics similar to melting layer) or convective updraft/downdrafts.

For some events, it is possible that no pronounced melting layer signature exists. As opposed to previous versions of the hydrometeor classification algorithm, data for melting layer detection is ingested from several elevation angles to maximize available signatures. Studies performed during the Joint Polarization Experiment (JPOLE) suggest that the optimal elevations for melting layer detection are between 4° and 9°. Model output may be utilized operationally to supplement the detection procedure or until sufficient radar statistics can be accumulated (e.g., Scharfenberg and Lakshmanan 2004).

3. Estimation of the bright band height and thickness for warm season rain events

Melting layer signatures were frequently observed in convective warm season storms during the JPOLE campaign in 2003. Prominent bright band signatures are detected in trailing stratiform regions behind squall lines. Figure 2 presents the results of polarimetric bright band detection for 4 warm season events observed during JPOLE (21 May, 4 June, 11 June, and 26 June, all 2003). Each image represents a bright band detection obtained using a single radar volume (volume starting from 1309 UTC, 1330 UTC, 0510 UTC, and 1720 UTC, respectively). Partial sounding information for temperature and dewpoint from soundings released near KOUN has been overlaid from the closest available time (00 UTC or 12 UTC).

Notable are the relatively low heights of the bottom of the melting layers in Fig. 2. Temperatures associated with bright band signatures typically fall between 1°C – 5°C and are centered at 2 – 3°C, in good agreement with several observations (e.g., Stewart et al. 1984, Willis and Heymsfield 1989, Pruppacher and Klett 1998, Ikeda and Brandes 2003). Slightly warmer temperatures in the later events (two lower panels) may be attributed to the large temporal mismatch between the time of the radar observation and the available soundings (approx. 5 hours).

As observed from the soundings, the bottom of the melting layer corresponds to approximately 5°C. Relative humidity observations in the layer below the freezing level for these events ranged between 85 – 95%. The freezing level was observed approximately 1 km above the bottom of the melting layer. This is consistent with observations of snow crystals falling several hundreds of meters below the melting layer into subsaturated air (e.g., Willis and Heymsfield 1989, Pruppacher and Klett 1998).

The azimuthal variability of melting layer signatures is also noteworthy. Relative differences in the bottom of this layer can exceed 0.4 km for these events. Most variability is attributed to differences in the large-scale temperature field. Local variability in the height and depth of the bright band appears to be linked to the location of the most intense convection (e.g., downdrafts, hail).

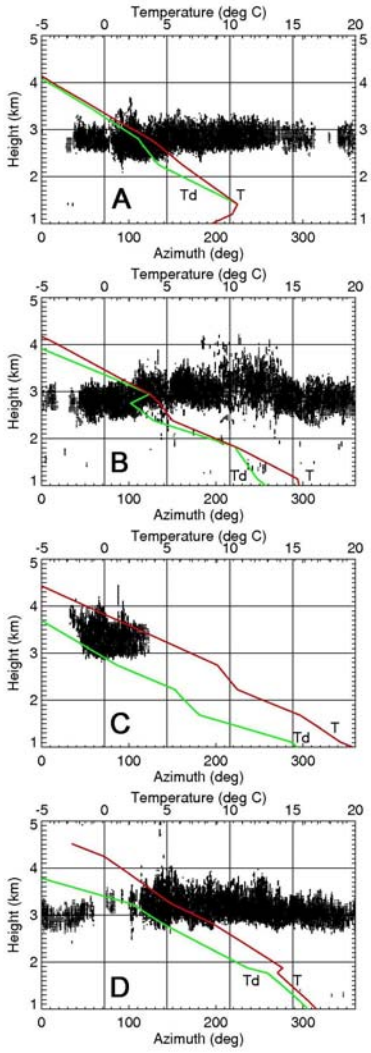

Fig. 2. Bright band detection for warm season events during 2003 on: (a) May 21, (b) June 4, (c) June 11, and (d) June 26. Temperature (red lines) and dewpoint (green lines) data from soundings launched near KOUN are overlaid on the plots.

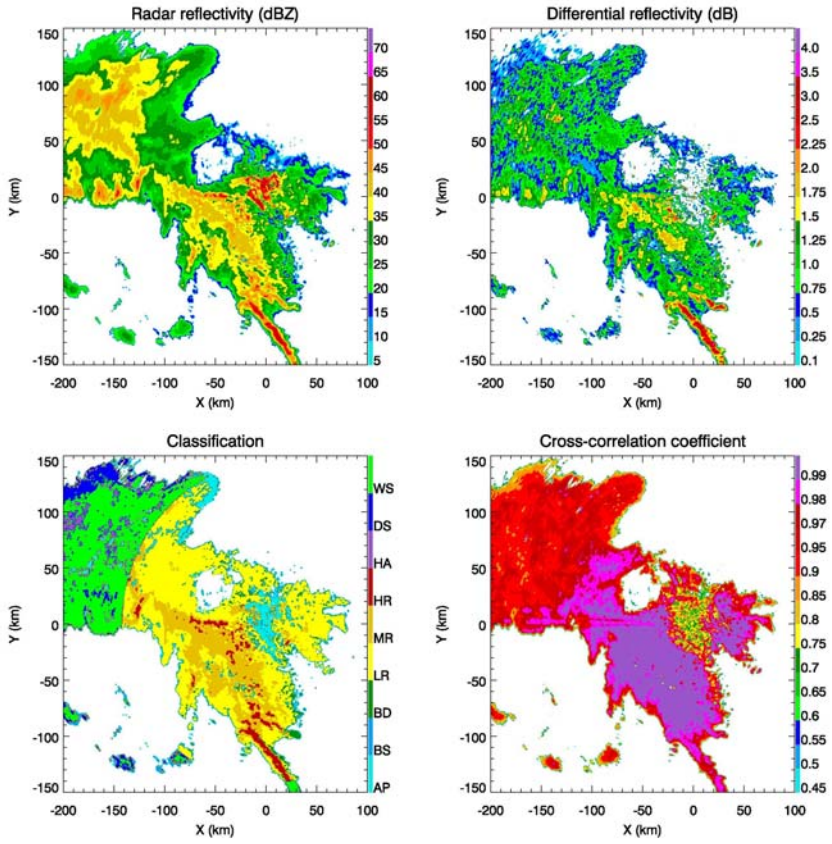

Fig. 3. Composite plot of polarimetric variables and the results of hydrometeor classification at the 0.5° elevation for the event on June 4, 2003 (1330 UTC). KOUN located at [0,0]. Classification scale represents light AP/ground clutter 'AP', biological scatteres 'BS', big drops 'BD', light rain 'LR', moderate rain 'MR', heavy rain/hail 'HR', hail 'HA', dry snow 'DS', and wet snow 'WS'.

Because of the relatively low bright band, potential bright band contamination of radar rainfall estimates made at 0.5° starts at 140 km from the KOUN radar even for these warm season events. This result has immediate implications for the accuracy of medium to long distance radar rainfall estimates at grazing angles.

4. Polarimetric hydrometeor classification and its implications for radar rainfall estimation

The 4 June 2003 event can be classified as a small MCS associated with a widespread region of moderate precipitation. The event included several intense embedded convective elements that produced small hail at the surface. As shown in previous sections, this case provides an excellent illustration of warm season bright band signatures. The event can also be utilized to highlight the implications of melting layer contamination for hydrometeor classification, data quality, and radar rainfall estimation.

Figure 3 shows several PPI images for different radar variables from the 0.5° elevation angle at 1330 UTC (KOUN located at [0,0]). Reflectivity factor does not exhibit pronounced bright band signatures. In contrast, the decrease of ρ_{HV} in the NW sector provides a clear indication of the bright band. The bright band signature for all radar variables is much more evident at the 4.5° elevation angle (Fig. 4). Notable is the lowering of Z_{DR} measurements above the melting layer associated with the presence of dry aggregated snow.

A fuzzy logic classification algorithm (e.g., Zrnic et al. 2001) was modified to incorporate the bright band detection routine. Once the height of the bottom of the bright band is determined, no designations of frozen hydrometeors are allowed below this height and rain designation is prohibited above this height. Figures 3 and 4 include the results of classification with this added routine.

The impact of bright band contamination on the quality of radar rainfall estimation for the rain event on 4 June 2003 is illustrated in Fig. 5, where one-hour rain

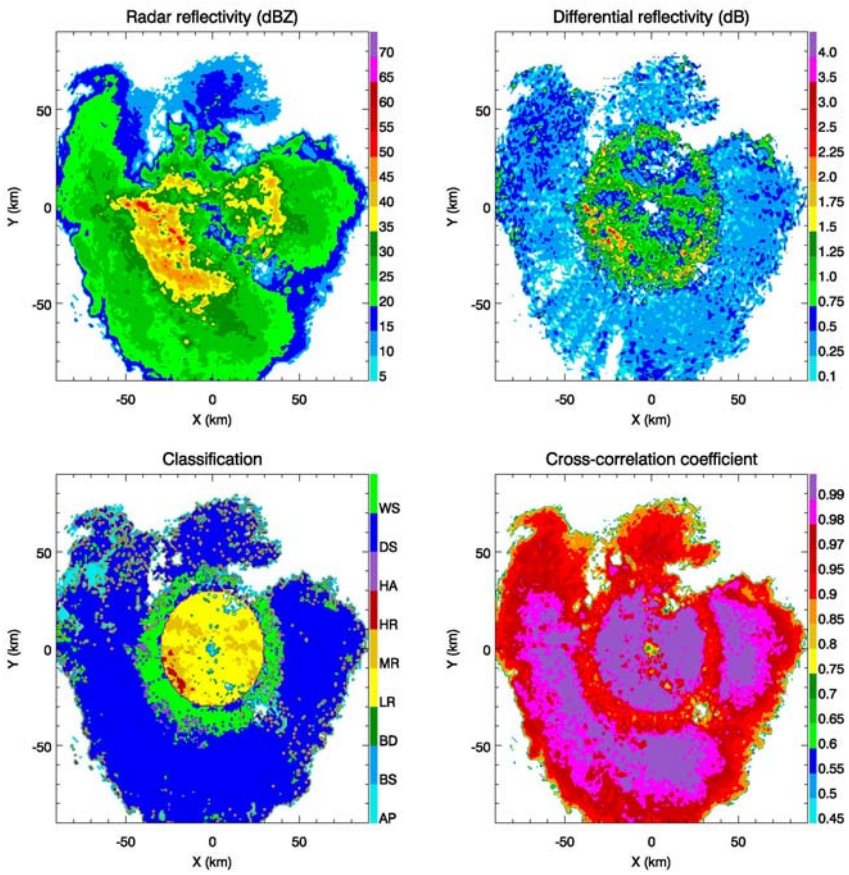

Fig. 4. As in Fig. 3, but for the 4.5° elevation.

accumulation maps obtained from the conventional R(Z) and polarimetric 'synthetic' algorithm described by Ryzhkov et al. (2003) are presented. Hourly gauge totals from the Oklahoma Mesonet are overlaid on the plots. Pronounced overestimation of rain by the conventional algorithm is evident in the areas of intense convection and bright band contamination (in NW sector).

There is a clear improvement in rainfall estimation with the use of polarimetric measurements, especially for the convective cells to the south of the KOUN radar. In the regions of bright band contamination, polarimetric rain estimates are very noisy due to enhanced oscillations of K_{DP} in the melting layer. However, if additional temporal/spatial averaging is performed, the polarimetric estimate exhibits significantly lower bias than the conventional counterpart.

5. Summary

This paper illustrates the use of polarimetric measurements for bright band detection, useful for several weather radar applications. The focus of this study is on detecting the bottom of the melting layer and its depth rather than on estimating the height of the freezing level.

For the warm season events presented in this paper, contamination occurs well below the freezing level. Soundings indicate a sizeable difference between the height of the freezing level and the bottom of the melting layer, where this contamination originates. Melting layer heights also exhibit a significant azimuthal dependence likely associated with the large-scale temperature field. This variability may be on the order of several hundreds of meters.

JPOLE observations show that during the warm season in Oklahoma, bright band contamination at the base radar tilt of 0.5° may occur at distances as close as 140 km from the radar. This observation has significant ramifications for data quality and hydrological applications, especially at large distance from the radar.

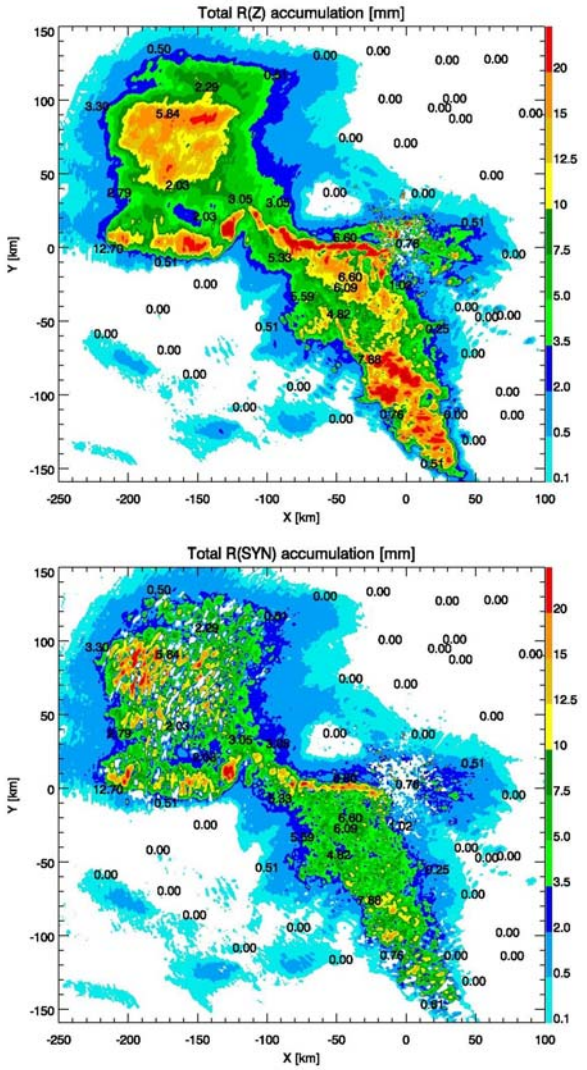

Fig. 5. Rainfall accumulation maps for 13 – 14Z on 4 June 2003 for a (a) conventional R(Z) and (b) polarimetric algorithm. Oklahoma Mesonet gauge accumulations are overlaid on the maps.

Acknowledgements

This work would not have been possible without the dedicated support from the NSSL and CIMMS / University of Oklahoma staff who maintain and operate the KOUN polarimetric WSR-88D.

References

Ikeda, K., and E.A. Brandes, 2003: Freezing-Level Determinations with Polarimetric Radar: Retrieval Model and Application, *Preprints, 31st Conf. Radar Meteor.*, Seattle, Washington, pp. 649 – 652.

Pruppacher, H.R., and J.D. Klett, 1998: *Microphysics of Clouds and Precipitation*, 2nd ed. Kluwer Academic Publishers, 954 pp.

Ryzhkov, A.V., S.E. Giangrande, and T.J. Schuur, 2003a: Rainfall Estimation with a Polarimetric Prototype of the Operational WSR-88D Radar, *Preprints, 31st Conf. Radar Meteor.,* Seattle, Washington, pp. 208 – 211.

Scharfenberg, K. A., and V. Lakshmanan, 2004: The Use of NWP Data in Polarimetric Hydrometeor Classification, *This Preprint CD Volume*, Hyannis, Massachusetts.

Stewart, R.E., J.D. Marwitz, and J.C. Pace, 1984: Characteristics through the Melting Layer of Startiform Clouds, *JAS*, 41, No. 22, pp. 3227 – 3237.

Willis, P.T., and A.J. Heymsfield, 1989: Structure of the Melting Layer in Mesoscale Convective System Stratiform Precipitation, *JAS*, 46, No. 18, pp. 2008 – 2025.

Zrnic, D.S., A.V. Ryzhkov, J. Straka, Y. Liu, and J. Vivekanandan, 2001: Testing a procedure for automatic classification of hydrometeor types. *J. Atmos. Oceanic Technol.*, 18, pp 892 – 913.